Pergamon

Tetrahedron 56 (2000) 6877–6885

TETRAHEDRON

Solid-State Chemistry of a Novel Carbapenem with a Releasable Sidechain

Örn Almarsson,* Randal A. Seburg, Danielle Godshall, Eric W. Tsai and Michael J. Kaufman

Merck Research Laboratories, Pharmaceutical Research and Development, West Point, PA 19486, USA

Received 23 February 2000; accepted 2 May 2000

Abstract—The solid-state chemistry of amorphous and crystalline forms of a novel cationic 1-β-methyl carbapenem antibiotic **2** is described. The lyophilized chloride salt of **2** (**2**·Cl) is amorphous and exhibits moisture-dependent β-lactam hydrolysis rates. Hydrolysis is concomitant with ejection of the sidechain naphthosultam moiety **4**. In the lyophilized solid (with 1.8% w/w water or less), a significant contribution from a Hofmann-like elimination reaction within the sidechain structure to give products **6** and **7** is observed. Another less significant elimination pathway involving loss of acetamide from the sidechain to form **8** is also operating at low residual moisture contents. Co-lyophilization of **2**·Cl with sucrose decreases the rate of the reactions within the sidechain as well as β-lactam hydrolysis, concomitant with a slight increase in the strength of the glassy lyophilized product based on modulated differential scanning calorimetry (MDSC). Kinetics of degradation of **2**·Cl lyophilized in the presence of 1% trisodium citrate and 50% weight of sucrose showed a 30–40% increase in overall initial rate of degradation at 25 and 40°C with increasing moisture from 0.3 to 1.1% residual water. Moisture enhances the stability of the *N*,*N*′-dialkyl 1,4-diaza[2.2.2]bicyclooctane (DABCO) sidechain structure in **2**·Cl, and this protective effect slightly offsets the increase in hydrolysis rate observed with increasing moisture. The crystalline benzenesulfonate trihydrate (**2**·$PhSO_3$) was characterized and found to have improved thermal stability in the solid state relative to the amorphous **2**·Cl, particularly in terms of the elimination pathway.

Introduction

Carbapenems are antibacterial agents of significant importance and clinical utility. A major goal in the antibacterial field is to discover and develop compounds that combat the emergence of methicillin resistance in S. Aureus (MRSA).[1] The synthesis of 1-β-methyl carbapenem **1** having anti-MRSA activity was described recently.[2] The compound was found to cause undesirable immunological reactions following multiple intravenous injections. These events were postulated to arise from the presence of the unusual aromatic and cationic sidechain, which may have played the role of a hapten to evoke an allergic response on repeated dosing. More recently, a strategy employing a releasable sidechain adjacent to the carbapenem has been shown to alleviate the immune reaction in this class.[3] We have found that upon β-lactam ring opening with a nucleophile compound **2** efficiently releases a naphthosultam sidechain **4** (Scheme 1). The rate of formation of **4** in solution is essentially equal to that of overall degradation of **2** in the pH range of 5 to 8. In this pH range, where one might consider formulating the compound for administration for reasons of solution stability, there is evidence for trace amounts (<1%) of the intermediate of hydrolysis with sidechain intact (**3** in Scheme 1).[4] This demonstrates that **3** is an unstable intermediate and prone to cleavage.[5] These observations are in agreement with the lack of immunological response to repeated doses of **2**.

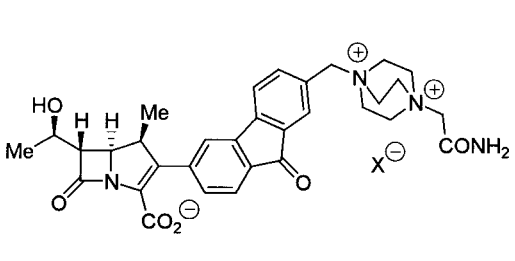

1

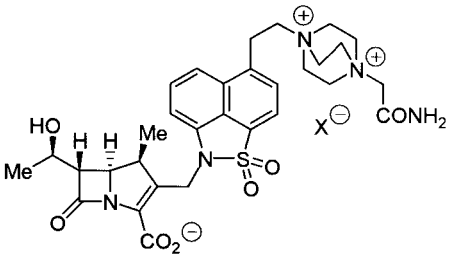

2

Keywords: carbapenems; antibiotics; hydrolysis; elimination reactions.

* Corresponding author. Fax: +1-215-652-5299; e-mail: orn_almarsson@merck.com

0040–4020/00/$ - see front matter
PII: S0040-4020(00)00509-3

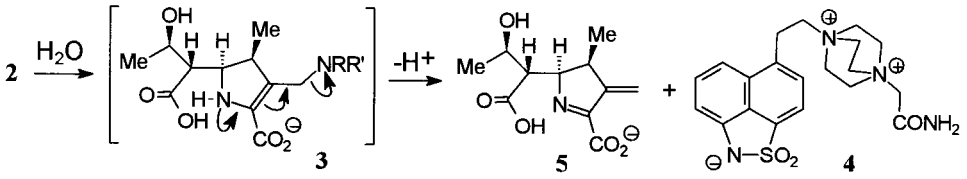

Scheme 1.

In this paper we report on the solid-state chemistry of **2** in two physical forms: (a) amorphous lyophilized chloride salt and (b) crystalline benzenesulfonate trihydrate. These forms are relevant in the quest for a stable pharmaceutical composition for long term storage, as solutions are too unstable to be viable marketed formulations. The relationship between β-lactam crystallinity and thermal stability is highlighted by the comparison of the solid state stability of the two forms. The quantitation of relative importance of two degradation pathways (one of which was unexpected) at given temperatures is provided as a function of residual moisture, additives and physical form.

Results and Discussion

The solid form of **2** that was initially isolated was the amorphous chloride salt (**2**·Cl), which contained significant residual water. The obvious question that arises relates to the dependence of thermal stability on hydration in the amorphous state. In Table 1 are compared stability data of **2**·Cl as provided with 11% w/w water, as well as reconstituted and re-lyophilized compound containing 1.8% w/w moisture, after 4 weeks of storage in sealed containers at 5, 25 and 40°C. Also included are stability data for lyophilized samples resulting from pH adjustment of the solution from pH 4.6 to 6.5 with NaOH prior to freeze-drying. These contained 1.4 and 0.3% residual moisture. The stability data were obtained by gradient HPLC of reconstituted solids in water. The data in Table 1 illustrate the effect of moisture on stability. Reduction of the moisture by over six-fold from 11 to 1.8% results in a decrease in the extent of degradation by over three-fold after 4 weeks at 5 and 25°C. The main pathway of degradation as determined by HPLC is hydrolysis with concomitant expulsion of naphthosultam **4**, as has been observed in aqueous solution of **2** (Scheme 1).[5] The reaction is slowed by at least two-fold over the six-fold moisture range. Comparing the data for 1.8 and 1.4% residual moisture, for which the pre-lyophilization pH of the latter was adjusted from 4.6 to 6.5, there is but a slight impact of pH adjustment on stability under all conditions of storage. The further reduction of residual moisture to 0.3% has a significant impact on stability of the freeze-dried solid at 5°C, although the increment of increased stability relative to the 1.4% residual moisture sample decreases successively at 25 and 40°C. Based on this information for the amorphous **2**·Cl, the approach indicated and henceforth employed was that of lyophilization into small unit dose vials with very low residual moisture (<1%) as a target to minimize degradation at 5 and 25°C.

Table 1. Solid-state stability of **2**·Cl as a function of residual moisture and pH adjustment after 4 weeks at 5, 25 and 40°C. Solids were kept in tightly capped glass vials (11% moisture samples) or vacuum-stoppered lyophilization vials (all other samples)

T (°C)	Change (Δ%)[a]	%H_2O (w/w)			
		11	1.8	1.4[b]	0.3[b]
5	**2**	−2.5	−0.79	−0.65	−0.062
	4	+2.2	+0.09	+0.11	–
25	**2**	−13	−4.3	−3.1	−2.4
	4	+11	+3.2	+2.1	+1.1
40	**2**	−17	−13	−10	−9.1
	4	+16	+11	+8.1	+6.3

[a] Δ%: Change in HPLC area percents from initials at 245 nm (see Experimental).
[b] Pre-lyophilization pH adjusted to 6.5.

A brief study of the photostability of the hydrated material (11% moisture) was conducted at approximately 30°C in capped borosilicate glass vials under fluorescent light (1300 lx). Exposed vials were compared with vials covered with aluminum foil under identical conditions. After 3 days exposure under broad spectrum visible light (approx. 100000 lx h), 86.1 and 95.1% of initial drug remained in an exposed sample and a foil-covered reference, respectively. While the main degradate in both samples was **4** by HPLC, numerous unidentified degradates not seen in the light-protected sample formed at low levels in the sample exposed to light. Subsequently **4** was found to be photosensitive in the absence of **2**; multiple light-induced products were formed and these have not been identified (data not shown). Although the photochemistry of the naphthosultams (**2** and **4**) appears to be rich, it was not studied further. Instead, samples of **2** were protected from light in order to focus on thermal reactions of **2** in the solid state.

It was noted in the measurement of stability of **2**·Cl that aqueous analyte solutions from reconstitution showed decreases in pH with increasing amounts of thermal stress regardless of initial pH adjustment. The downward pH drift correlated with increasing amounts of the hydrolysis product **4**. These observations are consistent with the formation of acidic products **4** and **5** according to Scheme 1. Evidence for the latter was found by LC/MS in the solvent front of the chromatographic profile. In addition, the disodium salt of **5** has been observed by ^{1}H NMR.[3b] Although not isolated for such studies, **5** is expected to be a reasonably strong organic diacid, whereas **4** was found to exhibit weak acidic character. A pK_a value for **4** of 5.23 was measured in dilute aqueous solution by spectrophotometric titration at 23°C. The value indicates that the liberated naphthosultam may offer some buffering in the pH range between 5 and 6, which is the range of maximum stability of the β-lactam function of **2** based on solution kinetics.[5] In contrast, **2** posesses a single pK_a around 3.2 by potentiometric titration and thus will not be self-buffering in the pH range of

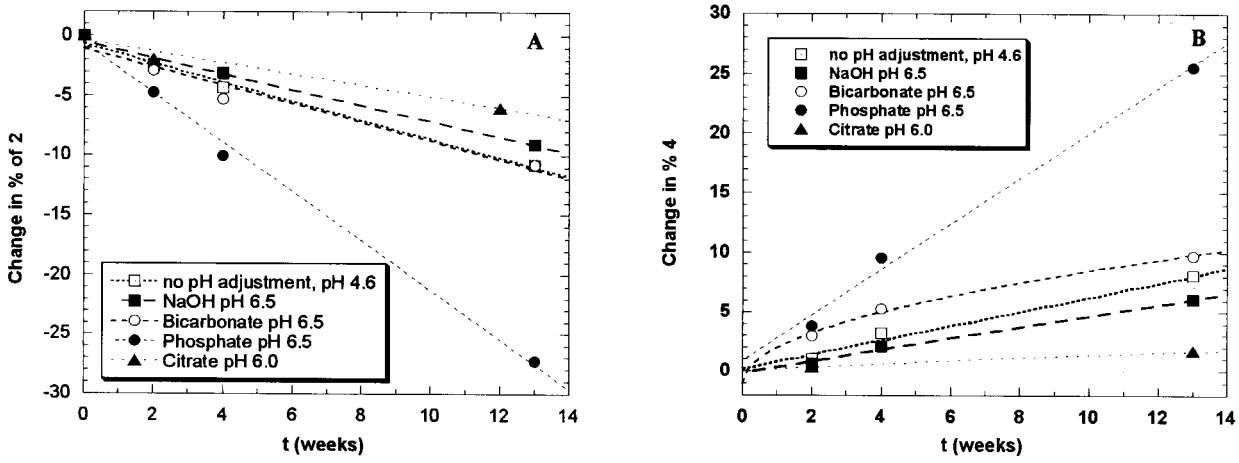

Figure 1. Effect of pH adjustment on the thermal stability of **2** over 13 weeks at 25°C. Residual moisture content in each was 1.4–1.8% w/w by Karl–Fischer titration, with the exception of the citrate buffered sample which had 1.0% w/w water. Panel A: Degradation of **2**. Panel B: Formation of **4**.

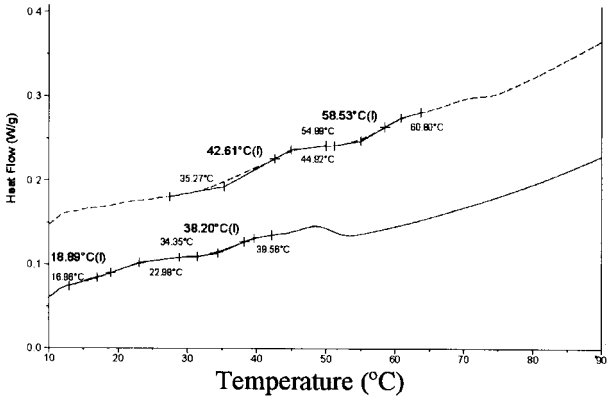

Figure 2. Modulated differential scanning calorimetry of **2**·Cl lyophilized in the presence and absence of sucrose at a heating rate of 4°C/min with 1°C/min sinusoidal modulation. Total heat flow traces are shown. Solid line: no sucrose added. Dashed line (offset in the *y*2-direction by +0.1 w/g): 50% weight sucrose added per weight of **2**.

maximum stability of the β-lactam. Based on these data and observations, the inclusion of a buffer seemed justified. The impact of pH on the initial rate of hydrolysis in the solid state was further addressed by lyophilizing solutions of **2** adjusted to pH 6.5 with disodium phosphate, sodium bicarbonate, and sodium hydroxide, as well as adjustment to pH 6.0 with sodium citrate. In Fig. 1 are shown the results of a thermal stability study over 13 weeks of storage at 25°C. From the data for the compositions containing 1.4–1.8% residual moisture, it is evident that pH adjustment with NaOH prior to freeze drying improves the thermal stability slightly as evidenced by the decrease in degradation rate from 0.80 to 0.66%/week based on linear fits of the data at 25°C. The effect of pH adjustment with sodium bicarbonate is negligible, possibly due to an offset in stability by buffer-catalyzed hydrolysis which is a well-documented phenomenon of β-lactams.[6] The addition of sodium phosphate buffer results in dramatic degradation of **2** and attendant formation of **4**, with an acceleration to 2.1%/week loss at 25°C, despite the lyophilized solid having a residual water content of approximately 1.4%. This is rationalized by the known propensity for disodium phosphate to crystallize on freezing, rendering freeze concentrated solutions more acidic (by several pH units).[7,8] As a result of the pH shift, acid-catalyzed hydrolysis increases significantly.[5] Citrate buffer appears to offer reasonable stability relative to the unbuffered lyophilizates of **2**·Cl.

It was reasoned that the thermal stability of **2**·Cl could be increased by addition of a saccharide component such as sucrose, as a means to dilute and strengthen the glassy matrix. In the absence of sucrose the lyophilized drug shows weak thermal transitions between 17°C and 38°C as shown by modulated differential scanning calorimetry (MDSC) measurements. The glass transition temperature of dry, amorphous sucrose is about 60°C.[9] The data in Fig. 2 indicate that the presence of sucrose (50% of the weight of drug) slightly strengthens the matrix by essentially eliminating the temperature transition at 17°C and by shifting the inflection at higher temperature from 38°C to approximately 43°C. There is also indication of a sucrose-like glass transition at 58°C. The chemical stability of **2** is enhanced by sucrose. In Table 2 are presented data from an experiment involving combinations of **2**·Cl with citrate and/or sucrose

Table 2. Solid-state stability of **2**·Cl, initial reconstitution pH, and reconstitution pH in water of stored lyophilized probe formulations in the presence and absence of trisodium citrate (1% w/w or 5 mM in the pre-lyophilization solution of **2**·Cl (100 mg/mL of **2**)) and/or sucrose (1:2 weight ratio vs. **2**) after 12 weeks at 5 and 25°C (Δ%: change in HPLC area percents from initials at 245 nm)

Formulation additive(s)	%H_2O (w/w)	Initial pH reconstit.	25°C		5°C	
			Δ% 2	Recon. pH	Δ% 2	Recon. pH
None	0.48	4.94	−6.4	4.54	−1.8	4.94
Citrate	0.22	5.76	−6.0	5.12	−1.5	5.76
Sucrose	0.32	4.94	−1.9	4.88	−0.46	4.94
Citrate+sucrose	0.74	6.15	−1.9	6.07	−0.34	6.15

Table 3. Solid-state stability of **2**·Cl in the presence of 1% w/w trisodium citrate and varying amounts of sucrose after 4 weeks at 25°C (Δ%: change in HPLC area percents from initials at 245 nm)

%sucrose[a]	%H_2O (w/w)	Δ% **2**	Δ% **4**	Δ% **6**[b]
10	0.15	−2.3	+0.76	+0.74
25	0.13	−1.5	+0.63	+0.62
50	0.11	−0.91	+0.51	+0.24

[a] Expressed as a percent weight of **2**.
[b] Elimination degradate; see structure below.

at 5 and 25°C. Based on the data a three-fold reduction in the degradation rate of **2** is observed at 25°C in the presence of the sucrose component. At 5°C the stability is observed to be improved by four-fold in the presence of sucrose. Based on comparison of the pH values on reconstitution after 12 weeks and at the initial time point, the role of citrate is simply to maintain pH within the range of maximum solution stability, and 1% w/w trisodium citrate does so reasonably when degradation remains <2%. It is concluded that sucrose is the critical component that improves the thermal stability of **2**·Cl by strengthening the lyophilized material.

The dependence of degradation rates on sucrose content in the lyophilized state was assessed by preparing additional formulations containing lower levels of sucrose (25% and 10% weight sucrose relative to the weight of **2**). The data in Table 3 illustrate the dependence of the degradation on sucrose content in lyophilized formulations of **2**·Cl.

The decrease in sucrose from 50% to 25% and 10% of weight relative to **2** causes a successive decrease in stability after 4 weeks at 25°C. In these formulations a significant decrease in the hydrolytic degradation is seen with increasing sucrose level. Saccharides have been found to catalyze hydrolysis of β-lactams in solution at intermediate and basic pH.[10] Such an effect appears to be absent in the solid-state chemistry of **2**·Cl; at the very least the catalytic effect of the carbohydrate is significantly offset by the strengthening and diluting effect of the sucrose matrix. A surprising finding in this experiment is that in addition to stabilization toward hydrolysis there is also a decrease in the degradate assigned structure **6** (by LC/MS and NMR). Degradate **6** is an intact β-lactam in which cleavage within the sidechain moiety has occurred. The alkene is proposed to result from a Hofmann-like elimination within the sidechain. LC/MS revealed the presence of the corresponding 1,4-diaza[2.2.2]bicyclo-octane (DABCO) N-acetamide (**7**) portion in the solvent front in the chromatographic traces. From the data in Table 3 it is evident that dilution with sucrose causes an almost proportional decrease in **6** after 4 weeks at 25°C. In addition to the formation of **6**, a less significant product of sidechain truncation **8** was observed (for which the fate of the acetamide is not known). It appears, therefore, that one function of sucrose is that of a water-mimicking stabilizer of the sidechain structure in which charge–charge repulsion of the dialkyl-DABCO dication becomes a significant driving force for degradation at very low moisture contents. The pathways for the degradation of **2** in the amorphous solid state are summarized in Scheme 2.

In order to explore the dependence of β-lactam hydrolysis and elimination reactions within the sidechain on moisture, the formulation in Table 4 was lyophilized to final water contents of 0.3 and 1.1%. In each case the pre-lyophilization pH was 6.0. The plots in Figs. 3–6 show the time courses of degradation of **2** and formation of hydrolysis product **4**, as well as elimination products **6** and **8**, in the lyophilized solids with 0.3 and 1.1% residual moisture at 40°C. Analysis of initial rates of degradation and formation of products was performed by linear regression of the initial phases of degradation at each moisture level and temperature. The extracted

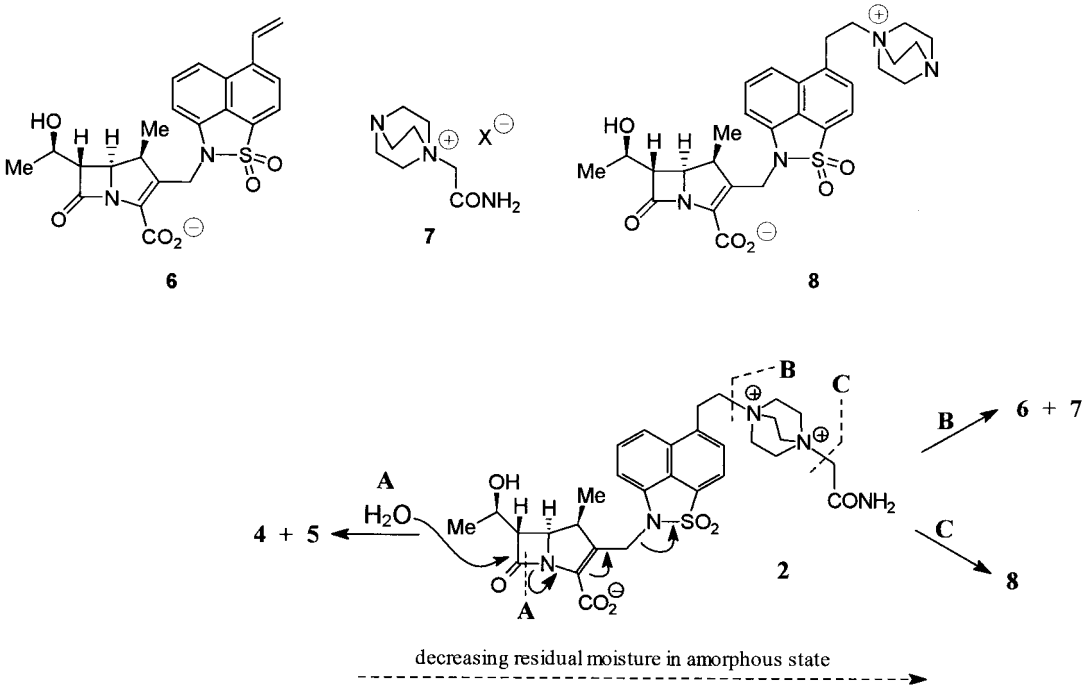

Scheme 2.

Table 4. Formulation (expressed as pre-lyophilization concentrate) of **2**·Cl for thermal stress study

Component	Amount
2 (as the free cation) (mg)	100.0
Citric acid anhydrous (mg)	0.060
Sodium citrate dihydrate (mg)	1.0
Sucrose (mg)	50.0
Water for injection (mL)	q.s. to 1.0

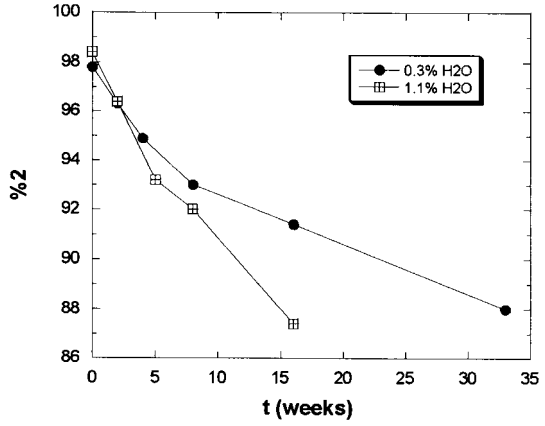

Figure 3. Time courses of degradation of lyophilized **2**·Cl (composition in Table 4), at 0.3 and 1.1% residual H_2O at 40°C.

rates are given in Table 5. Inspection of the initial rates reveals that the 1.4-fold increase in overall degradation rate resulting from increased moisture content from 0.3 to 1.1% is accounted for by (a) an increased rate of formation of **4** by 1.8-fold, and (b) a slightly smaller decrease of 30–40% in the rates of reactions in the sidechain. Based on the data, moisture is deleterious to the stability of the β-lactam ring but somewhat protective for the dicationic sidechain structure.

A detailed study of the temperature dependence of degradation of the formulation in Table 4, freeze-dried to 0.3% residual moisture, was performed. The time courses of degradation, shown in Fig. 7A, suggest biphasic kinetics at all temperatures except 60°C. At this temperature a linear decrease in **2** is observed with the available data. Linear fits

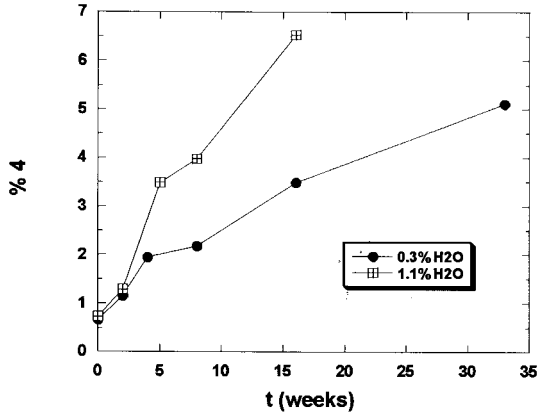

Figure 4. Time courses of formation of **4** in lyophilized **2**·Cl (composition in Table 4), at 0.3 and 1.1% residual H_2O at 40°C.

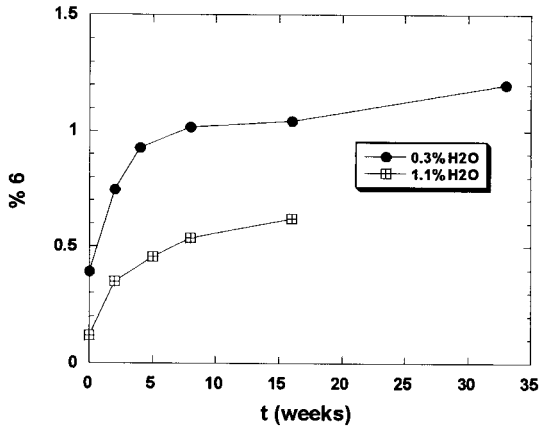

Figure 5. Time courses of formation of **6** in lyophilized **2**·Cl (composition in Table 4), with 0.3 and 1.1% residual H_2O at 40°C.

of the initial time points allowed a rough estimation of the temperature dependence of the first phase of reactions. The plot in Fig. 7B represents an attempt at Arrhenius treatment of the rates. The plot shows a reasonable fit of the data to the equation at 25–50°C with some deviation at 60°C. Thus, despite the presence of a thermal transition in the vicinity of 43°C (see Fig. 2) the formulation shows activation behavior that is in reasonable agreement with Arrhenius theory.

In the course of our studies with **2**·Cl, a crystalline benzenesulfonate salt of **2** (abbreviated **2**·$PhSO_3$) was discovered.

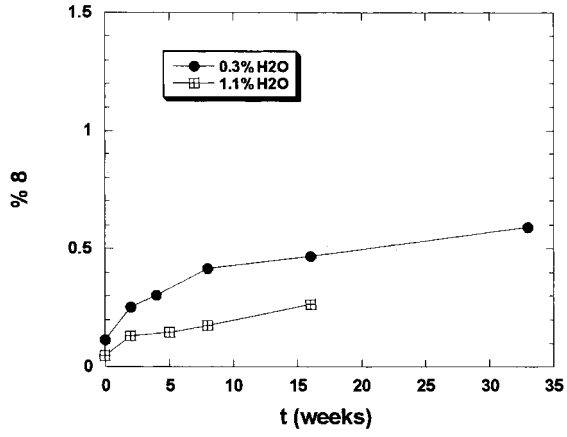

Figure 6. Time courses of formation of **8** in lyophilized **2**·Cl (composition in Table 4), with 0.3 and 1.1% residual H_2O at 40°C.

Table 5. Initial rates of overall degradation of carbapenem **2** and formation of degradates **4**, **6**, and **8** as a function of formulation moisture content at 40°C

Compound	Initial rates, ν (Δ%/week)[a]		Ratio, ν, 1.1%/ν 0.3%
	ν, 0.3% H_2O	ν, 1.1% H_2O	
2 (overall)	−0.73	−1.0	1.4
4	0.32	0.57	1.8
6	0.18	0.12	0.7
8	0.07	0.04	0.6

[a] Δ%: Change in HPLC area percents from initials at 245 nm.

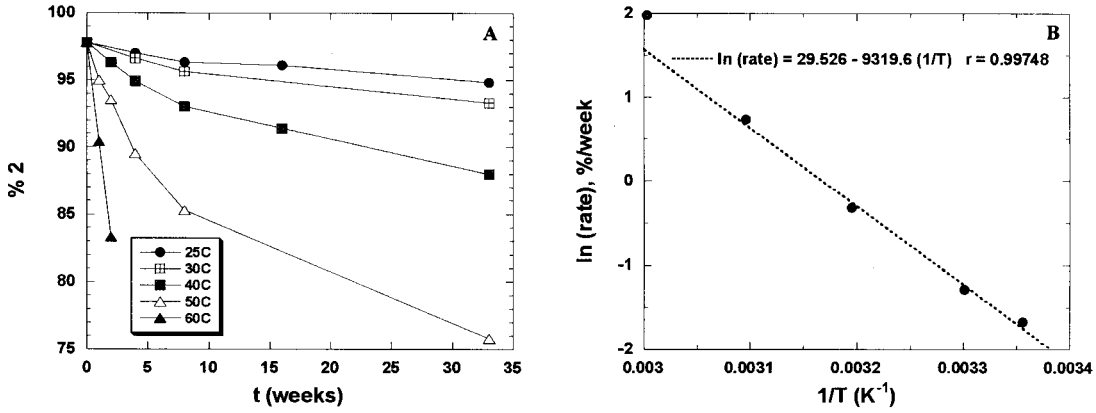

Figure 7. Dependence of degradation rate of **2**·Cl on temperature (0.3% residual H_2O). Panel A: Time courses of degradation of **2** at various temperatures. Panel B: Arrhenius plot of ln(Δ% **2**/week) vs. $1/T$ (K^{-1}).

In Fig. 8 is shown the X-ray powder diffraction pattern of **2**·$PhSO_3$ (Panel A), along with the thermal analysis (Panel B). The data reveal that this salt form is crystalline and contains 3 moles of water. The latter was indicated by thermogravimetric analysis (TGA, dashed line in Fig. 8B) and was confirmed by Karl–Fischer titration. TGA indicates that the water molecules are tightly bound. Differential scanning calorimetry (DSC) shows the presence of a melting endotherm at 149°C, without evidence of glass transition temperatures up to the melt. The melting is followed by a decomposition exotherm (solid line in Fig. 8B). In Fig. 9 are shown the time courses of thermal degradation of **2** and formation of **4** from crystalline **2**·$PhSO_3$. Comparison of the data with the stability profiles of lyophilized **2**·Cl (e.g. Fig. 7A and Table 5) indicates that despite the higher water content of the crystalline material, there is slower hydrolysis of **2**·$PhSO_3$ relative to that seen with **2**·Cl. For instance, at 40°C the rate of hydrolysis of **2**·$PhSO_3$ is roughly 0.35–0.4%/week, which is about half of the slowest degradation rate observed under the same conditions for formulated **2**·Cl (Table 5). In contrast to the degradation in the lyophilized formulation of **2**·Cl, there is negligible sidechain cleavage occurring at 40°C and only 0.6% of **6** formed at 60°C after 29 weeks. Instead, the reactivity of **2**·$PhSO_3$ in the solid state is mostly hydrolytic. The dominance of hydrolysis in the degradation of **2**·$PhSO_3$ is perhaps not surprising when one considers the three moles of water per **2** in comparison with the calculated 0.17 moles of water in the case of **2**·Cl at 0.3% residual moisture. The water molecules in **2**·$PhSO_3$ are likely to be fixed in the crystal structure, whereas in **2**·Cl the water molecules are not ordered. The context of the water molecules, in particular their dynamic mobility,[11] is therefore clearly important in determining the impact of the water in hydrolysis and elimination reactions of **2**. The data presented here follow the correlation of increased β-lactam stability with increased crystallinity observed by Pikal and coworkers for cephalosporins.[12] Based on comparison of data after 4 weeks at 40°C, the crystalline form of carbapenem **2** is approximately three times more stable than the amorphous **2** in a dry lyophilized formulation (Figs. 9 and 7, respectively).

The elimination to produce **6** with release of **7** is a significant thermal pathway of degradation in the amorphous state of **2**. Saunders Jr. et al. studied reactions of quaternary 2-arylethylammonium salts with a variety of bases in DMSO/aqueous solution, and have elucidated product regiochemistry as well as the kinetic mechanism.[13,14] A predominance of E_{1CB} character is evident in the kinetics of these solution phase reactions. The observed dependence of the reaction of **2** to form **6** on the presence of citrate is consistent with this mechanism. Using a 10-fold higher

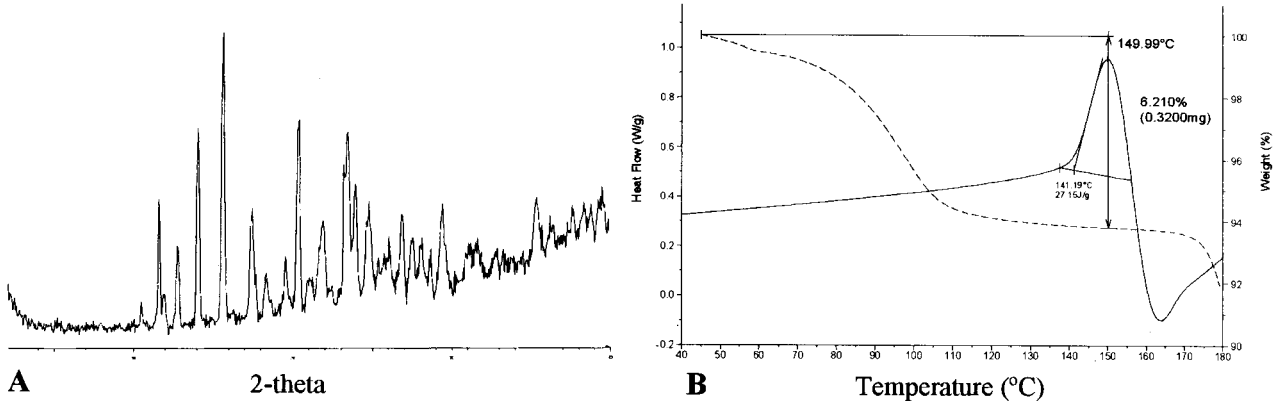

Figure 8. Characterization of the benzenesulfonate salt of **2**. Panel A: X-ray powder diffraction pattern of **2**·$PhSO_3$. Panel B: Thermogravimetric analysis (TGA;dashed line) and Differential Scanning Calorimetry (DSC; solid line) of **2**·$PhSO_3$ obtained at a heating rate of 10°/min.

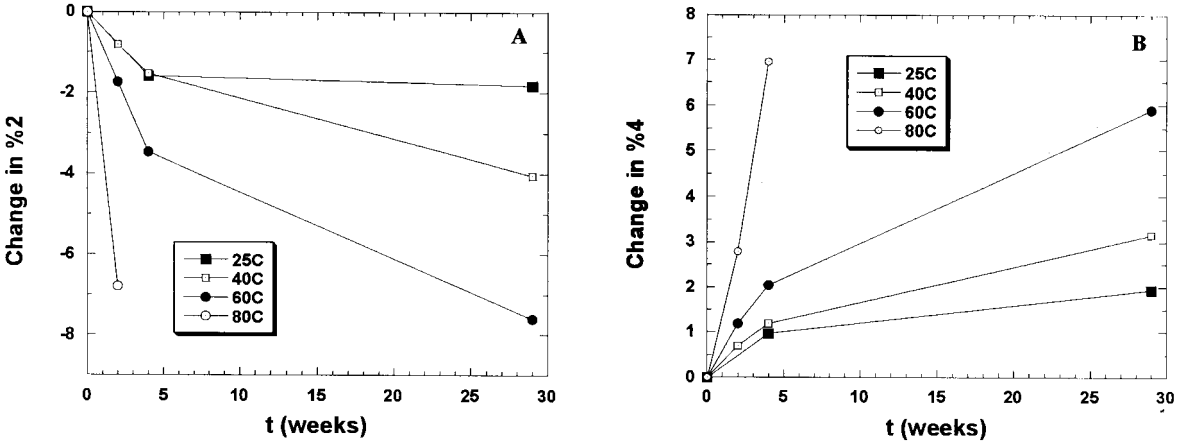

Figure 9. Dependence of degradation rate of crystalline **2**·$PhSO_3$ on temperature from 25 to 80°C. Panel A: Time courses of Δ% **2**. Panel B: Time courses of formation of **4**.

concentration of citrate than in the formula in Table 4, an increased level of **6** was observed in initial lyophilized samples (0.8% relative to 0.5% or less in general; data not shown). A complicating factor in this experiment was the observation of phase separation during freezing of the solution containing the larger amount of citrate. This points to an impending physical separation of **2**·Cl into an oily phase, an effect which may well be related to the overall chemical instability of this form of the drug on freeze-drying and thermal stress. For reference, 1,4-dialkyl DABCO salt derivatives have been recognized as surface active materials with unusual thermo-electric properties.[15]

A significant driving force for scission within the sidechain of **2** in the relatively anhydrous amorphous solid is likely to be the reduction in charge–charge repulsion within the *N*,*N*′-dialkyl DABCO unit. This effect plays a diminished role in the crystalline **2**·$PhSO_3$ trihydrate, perhaps due to the higher degree of order and more significant cationic charge stabilization by the crystal lattice waters in **2**·$PhSO_3$ relative to **2**·Cl. The slightly increased basicity of the benzenesulfonate counterion relative to chloride (based on solution pK_a values) may also offer stronger ionic interaction with the cations relative to chloride ion. The lack of observation of **8** in thermally stressed **2**·$PhSO_3$ is interesting, and suggests that chloride may be acting as a nucleophile displacing acetamide in **2**·Cl. Testing of this supposition was again complicated by observed phase separation during cooling of solutions of **2**·Cl which had been supplemented with NaCl. An 'oiling out' effect in the presence of salts is clearly a pervasive phenomenon of **2**·Cl.

As a final note, β-lactams are frequently encountered as stable crystalline solids containing hydration (prominent examples are amoxicillin trihydrate and imipenem hydrate, the carbapenem in Primaxin™) and yet are viable pharmaceuticals. This further illustrates the extent of stabilization afforded by the crystalline state and the importance of trapping the water molecules in a rigid lattice. A search of the Physician's Desk Reference 1999 edition uncovered eleven β-lactams that are hydrates of various stoichiometries (up to pentahydrate). These products are all labeled for room-temperature storage.[16]

Conclusion

We have described the solid-state chemistry of a novel carbapenem antibiotic **2** containing a hydrolytically releasable sidechain. The study highlights the significance of crystallinity and the nature of hydration to the chemical stability of β-lactams in the solid state.

Experimental

Samples of **2** chloride inner salt (**2**·Cl) were obtained from the departments of Medicinal Chemistry and Process Research at Merck (Rahway, NJ). The crystalline benzenesulfonate salt (**2**·$PhSO_3$) was prepared in Process Research. An authentic sample of **4** chloride salt was made available by Medicinal Chemistry. Sodium citrate dihydrate, citric acid, sodium phosphate, sodium bicarbonate, formamide and sucrose were purchased from Aldrich and used without further purification. Standard sodium hydroxide solutions for pH adjustment were purchased from Fisher. Doubly distilled water was used for preparation of buffers as well as NMR samples containing 90% v/v H_2O. Acetonitrile, methanol and 85% phosphoric acid were HPLC grade (Fisher). Dipotassium phosphate was obtained from Fisher. Karl–Fischer reagent and water standards (0.1 and 1.0%) were purchased from Riedel de Haen; the former was moisture-protected with activated 3A molecular sieve filters upon opening.

Lyophilization of formulations was performed on a FTS Systems Duradry lyophilizer. 3-mL capacity tubing vials were filled volumetrically with 0.20 mL of solution of **2** at 100 mg/mL of **2** and lightly capped with a two-legged West stopper. The vials were placed on the lyophilizer shelf and frozen at −45°C for one hour before a computer-programmed drying cycle was initiated. Primary drying was done at a fixed chamber pressure and temperature of 20 mtorr and −25°C, respectively. Two secondary drying steps of up to +30°C were employed. Vials were stoppered under vacuum within the chamber, removed from the lyophilizer and sealed prior to them being placed on stability stations.

Solutions for HPLC analysis were prepared in the following manner. After warming to room temperature, the vial containing the lyophilized formulation was carefully vented to atmosphere. Cold (5°C) diluent (20% CH_3CN/80% 0.005 M K_2HPO_4 buffer, pH 6.3) was pipeted into the vial to dissolve the lyo cake. The concentrated solution was quantitatively transferred to a volumetric flask and diluted to the mark with cold diluent. Resulting solutions were ca. 0.1 mg/ml. After transferring to HPLC vials, the solutions were maintained at 5°C on the HPLC autosampler tray, in order to minimize degradation before injection. Lyophilized samples that were checked for pH on reconstitution were diluted with water to 10 mg/mL concentration and their pH measured with a glass electrode standardized with Fisher reagent buffers. HPLC chromatography was performed on Hewlett Packard model 1090 and 1100, and Spectraphysics instruments with UV detection at 245 nm. Separation and elution was achieved with gradient acetonitrile/triethylammonium trifluoroacetate buffer (5 mM, pH 2.0) mixtures over a 250×4.6 mm Hypersil BDS C18 5 μm HPLC column at a flow rate of 1.0 mL/min. The gradient scheme involved 15–50% acetonitrile. Quantitation was achieved by integration in the software supplied by the LC chromatograph vendors using a standard of **2** the weight of which was adjusted for counterion and water content. The degradation data comprising Figs. 3–7 and Table 5 were obtained by HPLC using a Waters Alliance system or a Dionex GP40 gradient pump and Dionex AS3500 autosampler with a TSP UV2000 detector. Chromatography employed a 250× 4.6 mm GL Sciences Phenyl column, with gradient elution using a mobile phase of acetonitrile/phosphate buffer (5 mM, pH 6.3). The gradient profile ran from 5–50% acetonitrile. Data acquisition and quantitation was achieved using Multichrom version 2.11 (Lab Systems, Beverly, MA). In both HPLC methods the elution pattern in order of increasing retention time is **7**<**4**<**2**<**8**<**6**.

LC/MS experiments were performed on a Perkin–Elmer Series 200 LC and a Finnigan LCQ as the LC system and MS ion trap mass spectrometer, respectively. A gradient elution was used with ammonium acetate and acetonitrile as mobile phases. Both mass spectra and UV chromatograms along with UV spectra were recorded simultaneously. Mass spectra were acquired by using electrospray ionization at the positive mode. Degradate products **3**, **4**, **5**, **6**, **7**, and **8** were identified by LC/MS/MS. The following summarizes the degradate MS structural data in terms of mass to charge ratios and major CID fragments (the latter in parentheses): **3** *m/z* 642 (loss of CO_2 and CO_2+CO); **4** *m/z* 401 (loss of $-CONH_2$, $-CH_2CONH_2$, naphthosultam); **5** *m/z* 242 (loss of H_2O and CO_2); **6** *m/z* 455 (loss of H_2O and $CH_3CH(OH)CHCO$ or 86 Da); **7**; *m/z* 170 (loss of $-CONH_2$ and $-CH_2CONH_2$); **8** *m/z* 567 (loss of CO_2 and carbapenem moiety). Detailed structural analysis of these degradates are described in a separate publication.[5]

Karl–Fischer water titration was performed on a Brinkmann KF 737 Coulometer (Metrohm). 1:1 methanol–formamide stored in sealed vials over 3A molecular sieves was used to dilute lyophilized cakes by direct injection into the vials containing the cakes. The resulting solutions were then analyzed and corrected for the measured water content in blank diluent. X-Ray powder diffraction pattern was obtained on a Siemens D5000 diffractometer using a CuKα source and signal averaging over 0.05 2-theta data intervals. Thermal analyses (TGA and DSC) was performed on a TA instrument (models 2050 and 2920, respectively). A TGA ramp of 10°/min was employed with nitrogen purging. Modulated DSC was run in closed pans at 10°/min with 0.5°/s modulation.

Acknowledgements

The authors express gratitude to Drs Ronald Ratcliffe, Nobuyoshi Yasuda and Milton Hammond of Merck Research Laboratories for helpful discussions, Dr Ross Miller for providing the crystalline benzenesulfonate salt of **2**, and Drs Jean Kelly and Vincent Antonucci for stimulating discussions on stability and degradates. In addition, we would like to acknowledge Todd Armbruster for technical assistance, as well as expert LC/MS support and data interpretation by Drs Zack Zhao and Yunhui Wu.

References

1. Gold, H. S.; Mollering Jr., R. C. *Drug Therapy* **1996**, *335*, 1445–1453.
2. Yasuda, N.; Huffman, M. A.; Ho, G-J.; Xavier, L. C.; Yang, C.; Emerson, K. M.; Tsay, F-R.; Li, Y.; Kress, M. H.; Rieger, D. L.; Karady, S.; Sohar, P.; Abrahamson, N. L.; DeCamp, A. E.; Mathre, D. J.; Douglas, A. W.; Dolling, U.-H.; Grabowski, E. J. J.; Reider, P. J. *J. Org. Chem.* **1998**, *63*, 5438–5446.
3. (a) Rosen, H.; Hajdu, R.; Silver, L.; Kropp, H.; Dorso, K.; Kohler, J.; Sundelof, J. G.; Huber, J.; Hammond, G. G.; Jackson, J. J.; Gill, C. J.; Thompson, R.; Pelak, B. A.; Epstein-Toney, J. H.; Lankas, G.; Wilkening, R. R.; Wildonger, K. J.; Blizzard, T. A.; DiNinno, F. P.; Ratcliffe, R. W.; Heck, J. V.; Kozarich, J. W.; Hammond, M. L. *Science* **1999**, *283*, 703–706. (b) Ratcliffe, R. W.; Wilkening, R. R.; Wildonger, K. J.; Waddell, S. T.; Santorelli, G. M.; Parker Jr., D. L.; Morgan, J. D.; Blizzard, T. A.; Hammond, M. L.; Heck, J. V.; Huber, J.; Kohler, J.; Dorso, K. L.; St Rose, E.; Sundelof, J. G.; May, W. J.; Hammond, G. G. *Bioorg. Med. Chem. Lett.* **1999**, *9*, 679–684. (c) Humphrey, G. R.; Miller, R. A.; Pye, P. J.; Rossen, K.; Reamer, R. A.; Maliakal, A.; Ceglia, S. S.; Grabowski, E. J. J.; Volante, R. P.; Reider, P. J. *J. Am. Chem. Soc.* **1999**, *121*, 11261–11266.
4. For characterization of intermediates analogous to **3** in cephalosporins, see: Grabowski, E. J. J.; Douglas, A. W.; Smith, G. B. *J. Am. Chem. Soc.* **1985**, *107*, 267–268.
5. Zhao, Z.; Wang, Q.; Godshall, D.; Qin, X.-Z.; Tsai, E. W.; Reed, R. A.; Ip, D. P. Manuscript in preparation.
6. Bundgaard, H.; Hansen, J. *Int. J. Pharm.* **1981**, *9*, 273–283.
7. Larsen, S. S. *Arch. Pharm. Chem. Sci. Ed.* **1973**, *1* (3), 433–445.
8. Gomez, G. PhD Thesis, University of Michigan, 1995.
9. (a) Roos, Y.; Karel, M. *J. Food Sci.* **1991**, *56*, 266–267. (b) Hatley, R. H. M. *Pharm. Dev. Technol.* **1997**, *2*, 257–264. (c) Bonelli, P.; Schebor, C.; Cukierman, A. L.; Buera, M. P.; Chirife, J. *J. Food Sci.* **1997**, *62*, 693–695.
10. (a) Bundgaard, H.; Larsen, C. *Int. J. Pharm.* **1978**, *1*, 95–104. (b) Bundgaard, H.; Larsen, C. *Int. J. Pharm.* **1983**, *16*, 319–325.
11. For a key review on moisture effects on physical and chemical

stability in the solid state, see: Ahlneck, C.; Zografi, G. *Int. J. Pharm.* **1990**, *62*, 87–95.
12. (a) Pikal, M. J.; Lukes, A. L.; Lang, J. E.; Gaines, K. *J. Pharm. Sci.* **1978**, *67*, 767–773. (b) Pikal, M. J.; Lukes, A. L.; Lang, J. E. *J. Pharm. Sci.* **1977**, *66*, 1312–1316.
13. Brown, K. C.; Romano, F. J.; Saunders Jr., W. H. *J. Org. Chem.* **1981**, *46*, 4242–4246.
14. Dohner, B. R.; Saunders Jr., W. H. *J. Am. Chem. Soc.* **1986**, *108*, 245–247.
15. Terada, T.; Nogami, T.; Shirota, Y. *Bull. Chem. Soc. Jpn* **1989**, *62*, 5–10.
16. Physician's Desk Reference, Medical Economics Company Inc., 1999.